Electronic Supplementary Information (ESI)

Layered double hydroxide derived NiAl-oxide hollow nanospheres for selective transfer hydrogenation with improved stability

Zhengyi Pan,[a] Haibin Jiang,[a] Bingbing Gong,[b] Rong Luo,[a] Wenhua Zhang,[*b] and Guang-Hui Wang[*a]

[a] Department Key Laboratory of Biofuels, Qingdao Institute of Bioenergy and Bioprocess Technology, Chinese Academy of Sciences, Qingdao 266101, China

[b] Department Hefei National Laboratory for Physical Sciences at the Microscale, Department of Materials Science and Engineering, University of Science and Technology of China, Hefei 230026, China

[*] Corresponding author:

E-mail: whhzhang@ustc.edu.cn (W. Zhang); wanggh@qibebt.ac.cn (G.-H. Wang)

1. Experimental Details

Materials

Hexamethylenetetramine (HMT), 2,4-dihydroxybenzoic acid (DA) and Pluronic P123 were obtained from Sigma-Aldrich. Furfural (FFR), furfuryl alcohol (FOL), Na_2CO_3, NaOH, $Ni(NO_3)_2{\cdot}6H_2O$ and $Al(NO_3)_3{\cdot}9H_2O$ were purchased from Sinopharm Chemical Reagent Company. 5-hydroxymethylfurfural (HMF), 2,5-bis-(hydromethyl)-furan (BHMF), *trans*-cinnamaldehyde, cinnamyl alcohol, citral (cis- and trans- mixture), geraniol, nerol, 2-ethyl-2-hexenal, 2-ethylhex-2-enol and sodium oleate were acquired from Aladdin.

Synthesis of hollow polymer nanospheres (HPS)

The HPS sample was prepared according to the method reported previously with a slight modification.[1] In a typical preparation, 181 mg of DA and 0.071 g of HMT were dissolved in 60 mL of deionized water to form the solution A. 50 mg of Pluronic P123 and 73 mg of sodium oleate were dissolved in 20 mL of deionized water to form the solution B. Then, the solution B was added into the solution A under slow stirring at room temperature. After stirring for 15 min, the mixed solution was transferred into a Teflon-lined stainless-steel autoclave of 120 mL capacity, sealed and then maintained at 160 ^{o}C for 4 h. After cooling to room temperature, the product was collected by centrifugation at 14000 r.p.m. for 15 min, washed with the deionized water for 3 times, and dried at 50 ^{o}C under vacuum for 8 h.

Synthesis of pure NiO-t and solid Ni_3Al_1-t samples

Pure NiO-t nanoparticles and solid Ni_3Al_1-t were prepared by the same procedure

as mentioned in the main text, but in the absence of HPS and $Al(NO_3)_3 \cdot 9H_2O$ for pure NiO-t, and in the absence of HPS for solid Ni_3Al_1-t, respectively.

2. Catalyst characterization

Thermogravimetric analysis (TGA) was carried out on a NETZSCH STA 449F5 thermal analyzer under a dynamic air atmosphere (20 mL/min) in the temperature range between 25 and 700 °C, with a heating rate of 10 °C/min. X-ray diffraction (XRD) patterns were got on a Bruker D8 Advance powder diffractometer using Cu $K\alpha$ radiation (λ = 0.1541 nm) operated at 40 kV and 40 mA. Crystallite size (Dc) was calculated using the Scherrer equation, $Dc = K\,\lambda/(\beta \cos \theta)$, where the constant K is adopted as 0.9 here, λ is the wavelength of the X-ray radiation, β is the width of the peak at half-maximum, and θ is the Bragg angle. N_2 adsorption-desorption was performed on a Micromeritisc 3Flex instrument at -196 °C. The obtained h-NiAl catalysts were pretreated in vacuum at 200 °C for 6 h before measurement. The Brunauer-Emmett-Teller (BET) equation was used to calculate the specific surface area (S_{BET}). The pore volume (V_p) was estimated at a relative pressure of 0.99. The average pore diameter (d_p) was calculated using $d_p = 4V_p/S_{BET}$. The pore size distribution was determined by the Barret-Joyner-Halenda (BJH) method using the desorption branch of the isotherm. The sample reducibility and the interaction between Al^{3+} species and Ni-O sites were characterized by the H_2 temperature-programmed reduction (H_2-TPR) on a Micromeritics AutoChem II 2920 instrument. For this process, 30 mg precursor was loaded into a quartz U-shaped tube and reduced

in a 10 vol % H_2/Ar flow (20 mL/min) at a heating rate of 10 °C/min. The hydrogen consumption was determined by a thermal conductivity detector (TCD). The NH_3 or CO_2 temperature-programmed desorption (NH_3/CO_2-TPD) characterization was conducted on the same equipment as with H_2-TPR. 100 mg catalyst was purged with an Ar or He flow (20 mL/min) at 250 ^oC for 1 h and then cooled to 100 ^oC. After NH_3 or CO_2 adsorption until saturation, the sample was flushed with an Ar or He flow (20 mL/min) to remove the physically adsorbed NH_3 or CO_2. Subsequently, NH_3/CO_2-TPD was implemented at a heating rate of 5 ^oC/min with a TCD to detect the desorbed NH_3 or CO_2.

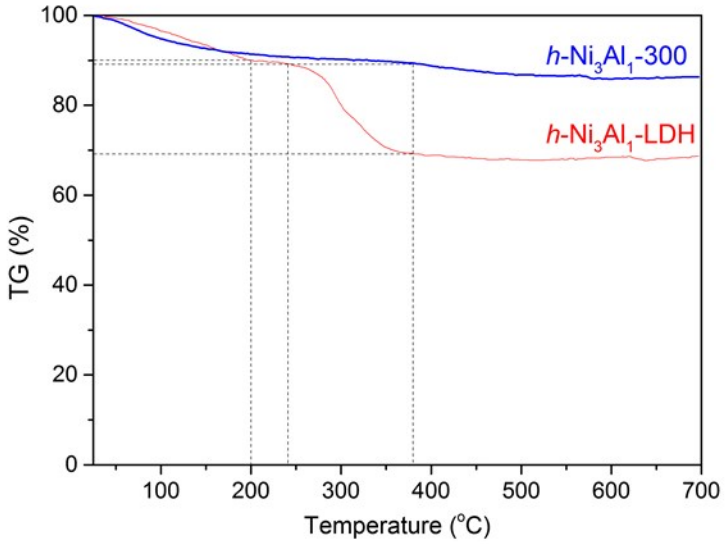

Fig. S1 TGA curves of HPS@Ni_3-Al_1-LDH and *h*-Ni_3Al_1-300.

As shown in Fig. S1, for HPS@Ni_3Al_1-LDH, the weight loss below 200 °C is due to the removal of physical adsorbed and bond water;[2] the weight loss in the range of 240~375 °C is mainly due to the removal of HPS template; almost no weight loss occurs when the temperature is above 375 °C. In contrast, for *h*-Ni_3Al_1-300, there is almost no weight loss in the range of 240~375 °C, indicating that the HPS template can be removed completely after calcination at 300 °C for 5 h (*h*-Ni_3Al_1-300).

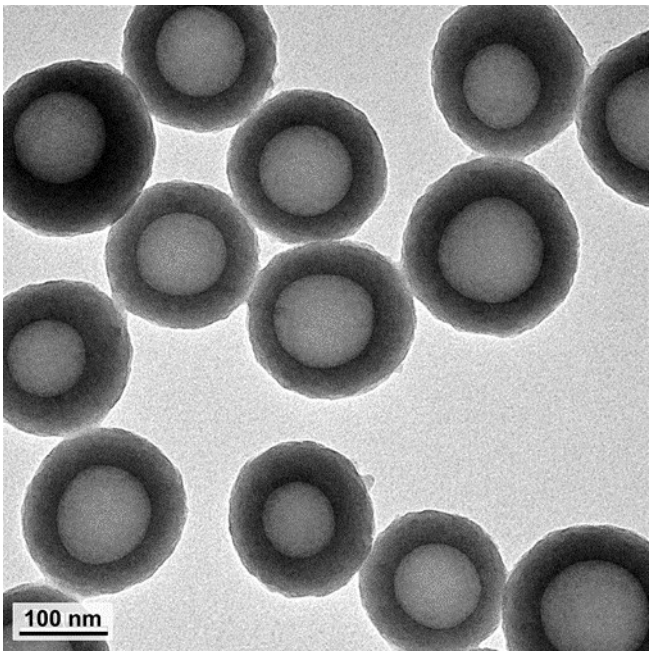

Fig. S2 TEM image of HPS with a diameter of about 185 nm.

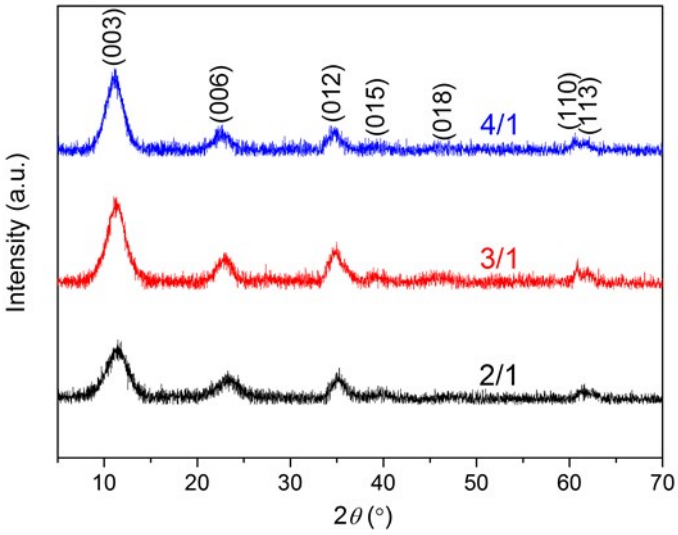

Fig. S3 XRD patterns of different HPS@Ni_x-Al_y-LDH samples (x/y= 4/1, 3/1 or 2/1), indicating the existence of LDH structure in all samples. Note: the number without parentheses on the curve indicates Ni/Al molar ratio.

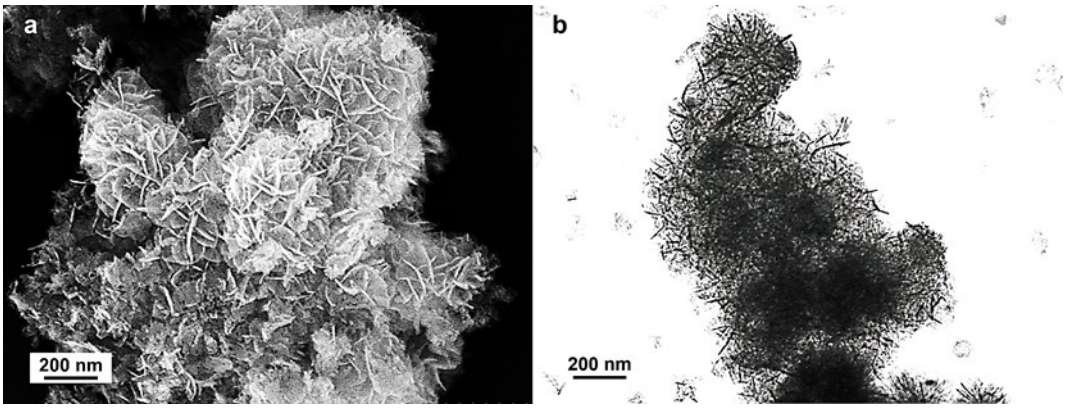

Fig. S4 (a) SEM and (b) TEM images of Ni_3Al_1-800 without using HPS as template during synthesis.

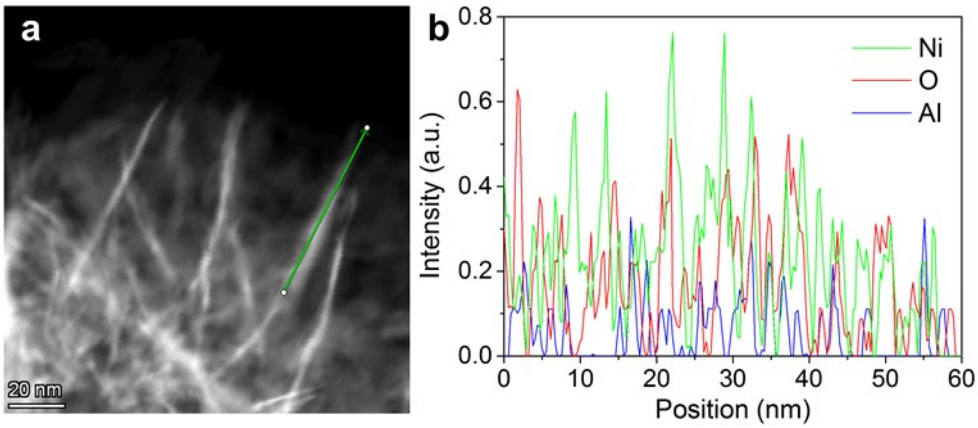

Fig. S5 (a) STEM image and (b) corresponding EDS line scanning profile (green line in a) of Ni, O and Al elements on *h*-Ni_3Al_1-800.

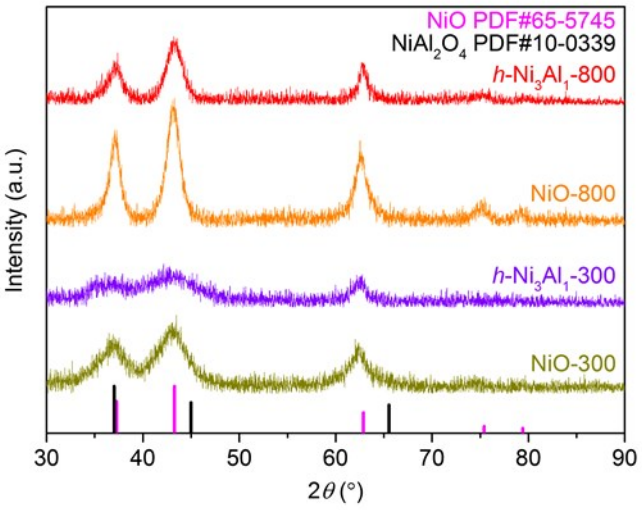

Fig. S6 XRD patterns of *h*-Ni_3Al_1-t and NiO-t.

Table S1 the particle size of NiO (*Dc*) using the Scherrer equation ($Dc = K\lambda/(\beta \cos\theta)$).

Catal.	*K*	λ	2θ (°)	β (°)	*Dc* (nm)
h-Ni_3Al_1-1000	0.9	0.1541	43.287	0.822	10.4
h-Ni_3Al_1-900	0.9	0.1541	43.238	1.613	5.3
h-Ni_3Al_1-800	0.9	0.1541	43.282	1.901	4.5
spent *h*-Ni_3Al_1-800	0.9	0.1541	43.306	1.901	4.5
h-Ni_3Al_1-700	0.9	0.1541	43.182	1.988	4.3
h-Ni_3Al_1-600	0.9	0.1541	43.266	2.036	4.2
h-Ni_3Al_1-500	0.9	0.1541	43.413	2.593	3.3
h-Ni_3Al_1-300	0.9	0.1541	43.801	4.760	1.8
spent *h*-Ni_3Al_1-300	0.9	0.1541	43.685	4.758	1.8
Ni_3Al_1-800	0.9	0.1541	43.257	1.782	4.8
h-Ni_2Al_1-800	0.9	0.1541	43.269	2.036	4.2
h-Ni_4Al_1-800	0.9	0.1541	43.300	1.711	5.0
NiO-800	0.9	0.1541	43.230	1.316	6.5
NiO-300	0.9	0.1541	43.175	2.758	3.1
spent NiO-300	0.9	0.1541	43.101	2.757	3.1
Al_2O_3-800	0.9	0.1541	45.575	1.540	5.6

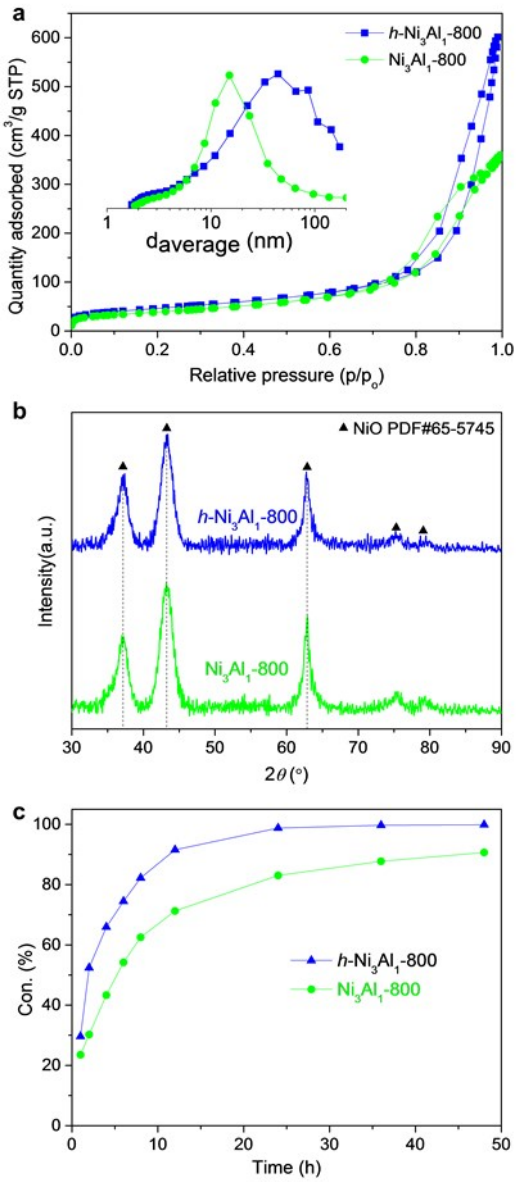

Fig. S7 (a) N_2 sorption isotherms (insert: pore size distributions) and (b) XRD patterns of *h*-Ni_3Al_1-800 and Ni_3Al_1-800. (c) Selective transfer hydrogenation of FFR over *h*-Ni_3Al_1-800 and Ni_3Al_1-800. Reaction conditions: 1.0 mmol FFR, 10 mL 2-propanol, 80 mg catalyst, 120 °C.

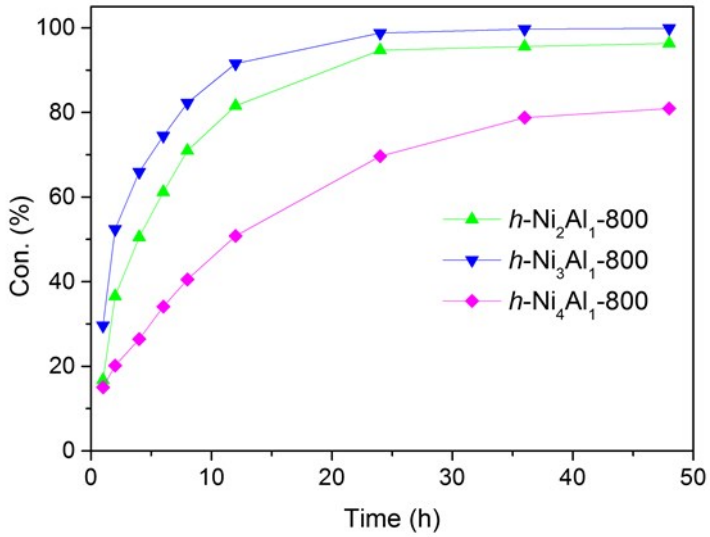

Fig. S8 Selective transfer hydrogenation of FFR to FOL over different *h*-Ni_xAl_y-800 (x/y= 2/1, 3/1 or 4/1) catalysts. Reaction conditions: 1.0 mmol FFR, 10 mL 2-propanol, 80 mg catalyst, 120 ^oC.

Table S2 STH of FFR to FOL over different metal oxides in literature.

Entry	Catal.	Mass ratio[a]	$C_{initial}$[b] (mol L^{-1})	T(°C)	t(h)	Conv.(%)	Sel.(%)	TOF(h^{-1})[c,d]	Ref.
1	La_2O_3	0.8	0.03	180	3	41	75	**0.4** *(41%, 3h)*	3
	Fe_2O_3					38	60	**0.2** *(38%, 3h)*	
	$LaFeO_3$_NA					90	94	**0.6** *(90%, 3h)*	
					2	75	85	**0.8** *(75%, 2h)*	
					1	70	80	**1.4** *(70%, 1h)*	
				200	3	100	82	**0.6** *(100%, 3h)*	
				160		71	75	**0.4** *(71%, 3h)*	
				120		18	39	**0.1** *(18%, 3h)*	
		1.2	0.04	180		68	98	**0.6** *(68%, 3h)*	
		1.4	0.05			67	85	**0.7** *(67%, 3h)*	
		2.0	0.07			55	86	**0.9** *(55%, 3h)*	
2	Fe_3O_4	3.2	0.2	180	4	57	95	**0.2**[e]	4
	$CoFe_2O_4$					73	97	**0.3**[e]	
	$NiFe_2O_4$					95	95	**0.7**[e]	
3	γ-Fe_2O_3 @HAP	4.8	0.07	180	3	40	90	**1.1** *(40%, 3h)*	5
		2.4				65	92	**0.9** *(65%, 3h)*	
		1.2				78	97	**0.5** *(78%, 3h)*	
		2.4		160		50	95	**0.7** *(50%, 3h)*	
				140		33	82	**0.4** *(33%, 3h)*	
				120		15	81	**0.2** *(15%, 3h)*	
4	MgO	10	0.55	120	5	20	70	**0.2** *(20%, 5h)*	6
				150		76	71	**0.6** *(76%, 5h)*	
				170		100	74	**0.8** *(100%, 5h)*	
	Al_2O_3-450					75	58	**1.6** *(75%, 5h)*	
	ZrO_2					75	53	**1.9** *(75%, 5h)*	
	ZnO					74	65	**1.3** *(74%, 5h)*	
5	NiO(P)-300	4.8	0.2	120	1	73	97	**2.7**[e]	7
	Commercial NiO					18	96	**0.7**[e]	
	NiO-300					63	91	**2.3**[e]	
	NiO(P)-400					11	93	**0.4**[e]	

Table S2 (contd.)

Entry	Catal.	Mass ratio[a]	$C_{initial}$ [b] (mol L^{-1})	T(°C)	t(h)	Conv.(%)	Sel.(%)	TOF(h^{-1})[c,d]	Ref.
6	MgO	3.2	0.2	150	1	21	77	**0.3** *(21%, 1h)*	8
	TiO_2					29	57	**0.8** *(29%, 1h)*	
	Cr_2O_3					21	60	**1.1** *(21%, 1h)*	
	Fe_2O_3					29	57	**1.6** *(29%, 1h)*	
	ZrO_2					32	80	**1.2** *(32%, 1h)*	
	NiO					54	97	**1.3** *(54%, 1h)*	
7	*h*-Ni_3Al_1-800	3.2	0.2	150	1	48	>99	**1.1** *(48%, 1h)*	This work

[a] Mass ratio of furfural to catalyst. [b] Initial molar concentration of FFR. [c] TOF was calculated based on the content of metallic oxides. [d] Calculated based on the data in literature; the numbers in parentheses are the reaction time and the conversion for TOF estimation. [e] Mentioned in literature.

In this work, even based on the NiO content, the TOF value over the *h*-Ni_3Al_1-800 still reached 1.1 h^{-1}, which is in the same order of magnitude with the values reported in literature. More importantly, the *h*-Ni_3Al_1-800 can be recycled at least 12 times without loss of activity, indicative of its higher stability for STH reaction than those reported in literature.

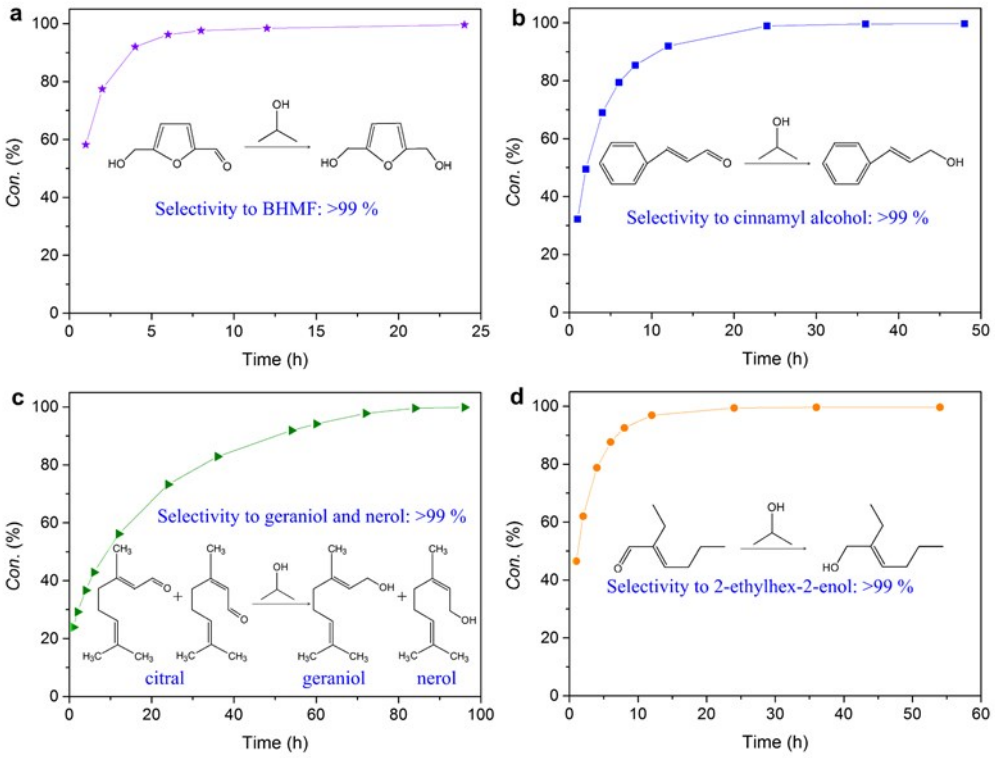

Fig. S9 Catalytic performances of *h*-Ni_3Al_1-800 for selective transfer hydrogenation of (a) HMF to BHMF, (b) *trans*-cinnamadehyde to cinnamyl alcohol, (c) citral to geraniol or nerol and (d) 2-ethyl-2-hexenal to 2-ethylhex-2-enol. Reaction conditions: 0.5 mmol substrate, 5 mL 2-propanol, 80 mg catalyst, 120 ^{o}C.

Table S3 Ni 2p XPS results of different catalysts.

Catal.	Ni^{2+} (NiO)			$Ni^{\delta+}$ (Ni-O-Al, $2< \delta < 3$)			Ni^{3+} (Ni_2O_3 or NiOOH)			O^{2-} (NiO)	O^{2-} (Ni-O-Al)	O^{2-} (Ni_2O_3 or NiOOH)
	Binding energy (eV)	FWHM[c] (eV)	Percent (%)	Binding energy (eV)	FWHM[c] (eV)	Percent (%)	Binding energy (eV)	FWHM[c] (eV)	Percent (%)	Binding energy (eV)	Binding energy (eV)	Binding energy (eV)
h-Ni_3Al_1-1000	854.4	2.06	27.5	855.6	2.05	29.2	856.8	2.11	43.3	--	530.8	--
h-Ni_3Al_1-800	854.4	2.02	20.3	855.6	2.15	60.1	856.8	2.13	19.6	--	530.8	--
Spent *h*-Ni_3Al_1-800[a]	854.4	2.02	19.8	855.6	2.10	62.2	856.8	2.10	17.9	--	530.8	--
h-Ni_3Al_1-500	854.4	2.02	31.3	855.4	2.05	29.7	856.5	2.11	39.0	--	530.6	531.4
h-Ni_3Al_1-300	854.4	1.90	2.3	855.2	2.06	26.6	856.2	2.13	71.1	--	530.5	531.5
Spent *h*-Ni_3Al_1-300[b]	854.7	1.95	10.7	855.5	2.02	38.8	856.7	2.12	50.5	--	530.5	531.5↓[d]
NiO-800	854.4	2.02	36.0	--	--	--	856.2	2.12	64.0	529.9	--	531.9
NiO-300	854.2	2.02	32.6	--	--	--	855.8	2.12	67.4	529.4	--	531.2
Spent NiO-300[b]	854.3	2.02	42.0	--	--	--	856.0	2.12	58.0	529.7	--	531.3↓[d]

[a] Recycled 12 times. [b] Recycled 6 times. [c] The full width at half-maximum (FWHM). [d] ↓ indicates that the amount of O^{2-} species in Ni_2O_3 or NiOOH after recycling decreases.

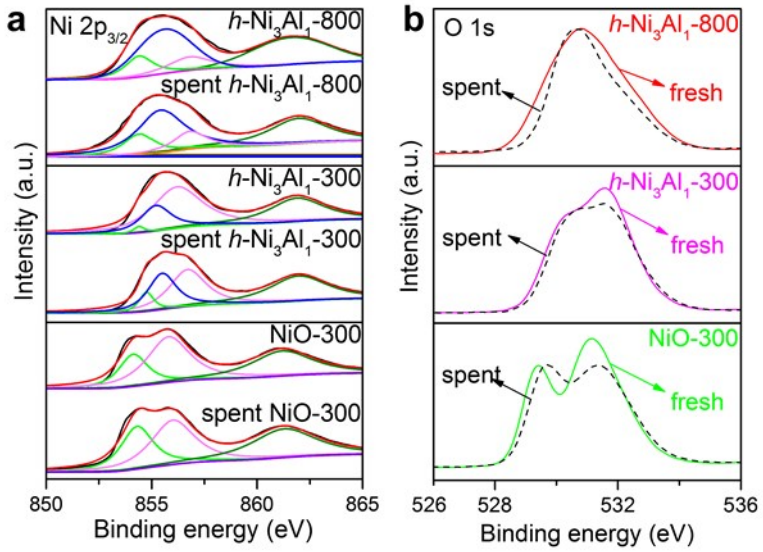

Fig. S10 (a) Ni $2p_{3/2}$ and (b) O 1s XPS spectra of NiO and *h*-Ni_3Al_1 catalysts before and after recycling (12 times for *h*-Ni_3Al_1-800, 6 times for *h*-Ni_3Al_1-300 and NiO-300, respectively).

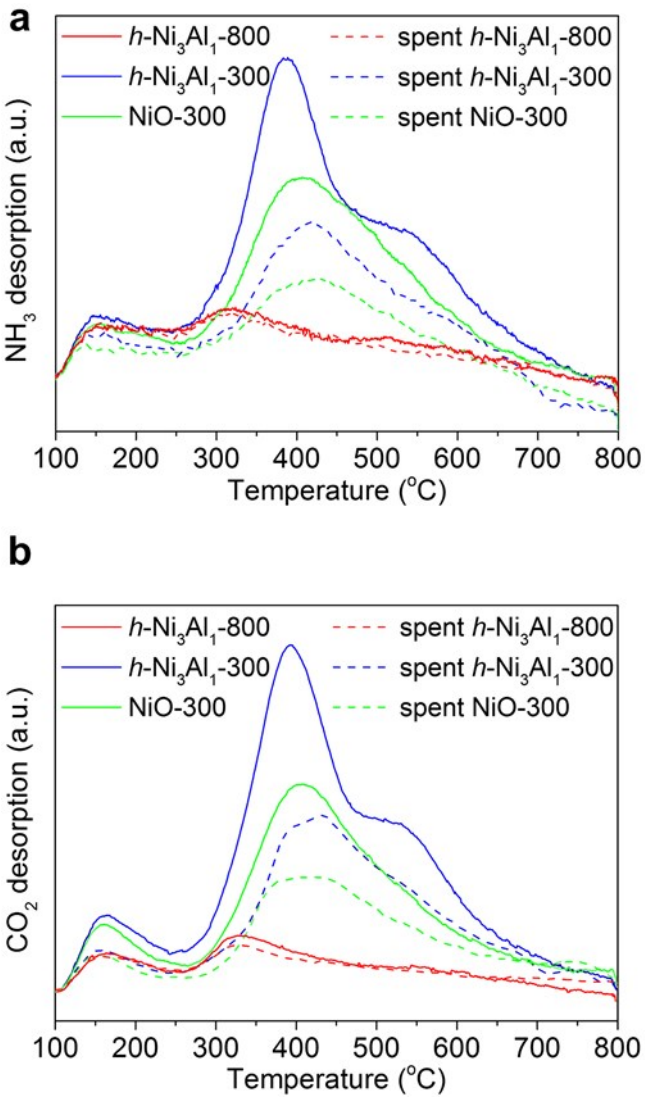

Fig. S11 a) NH_3-TPD and b) CO_2-TPD profiles of the catalysts before and after recycling.

Table S4 Acid-base properties of different catalysts.

Catal.	Acid site density[a] ($mmol_{NH3}\ g_{cat}^{-1}$)	Base site density[b] ($mmol_{CO2}\ g_{cat}^{-1}$)
h-Ni_3Al_1-1000	0.6	0.5
h-Ni_3Al_1-800	1.3	1.4
h-Ni_3Al_1-500	2.0	2.4
h-Ni_3Al_1-300	3.9	5.3
NiO-800	0.0	0.2
NiO-300	3.0	3.5
Spent *h*-Ni_3Al_1-800[c]	1.3	1.3
Spent *h*-Ni_3Al_1-300[d]	2.2	2.7
Spent NiO-300[d]	1.7	2.1

[a] Obtained from NH_3-TPD. [b] Obtained from CO_2-TPD. [c] Recycled 12 times. [d] Recycled 6 times.

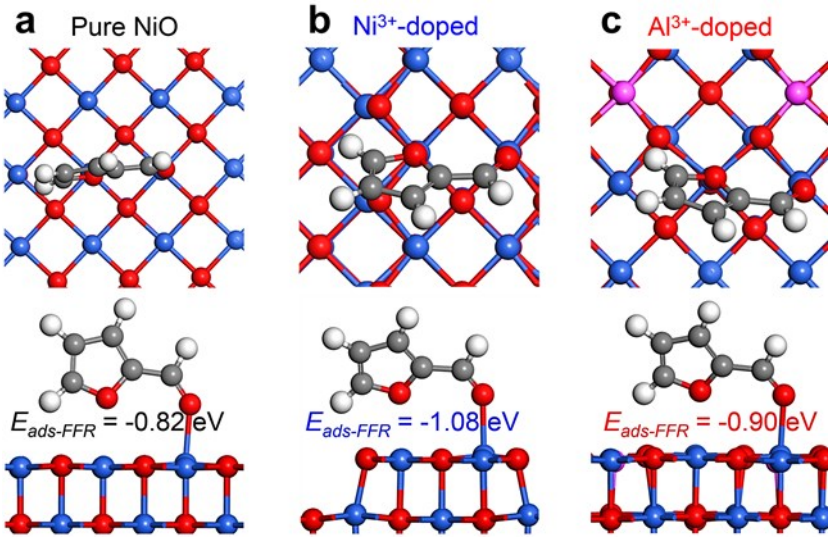

Fig. S12 The top and side view of the most stable adsorption configuration of FFR on (a) pure NiO(200), (b) Ni^{3+}-doped Ni(200) and (c) Al^{3+}-doped NiO(200). The blue, pink, red, gray and white spheres represent Ni, Al, O, C and H atoms, respectively.

Notes and references

1 G. H. Wang, J. Hilgert, F. H. Richter, F. Wang, H. J. Bongard, B. Spliethoff, C. Weidenthaler and F. Schuth, *Nat. Mater.*, 2014, **13**, 293-300.

2 X. Li, L. Zheng and Z. Hou, *Fuel*, 2018, **233**, 565-571.

3 P. Xiao, J. Zhu, D. Zhao, Z. Zhao, F. Zaera and Y. Zhu, *ACS Appl. Mater. Interfaces*, 2019, **11**, 15517-15527.

4 J. He, S. Yang and A. Riisager, *Catal. Sci. Technol.*, 2018, **8**, 790-797.

5 F. Wang and Z. Zhang, *Chem. Eng.*, 2017, **5**, 942-947.

6 N. S. Biradar, A. M. Hengne, S. S. Sakate, R. K. Swami and C. V. Rode, *Catal. Lett.*, 2016, **146**, 1611-1619.

7 J. He, M. R. Nielsen, T. W. Hansen, S. Yang and A. Riisager, *Catal. Sci. Technol.*, 2019, **9**, 1289-1300.

8 J. He, L. Schill, S. Yang and A. Riisager, *ACS Sustainable Chem. Eng.*, 2018, **6**, 17220-17229